pubs.acs.org/Biomac

Article

# A Single Enzyme Mediates the "Quasi-Living" Formation of Multiblock Copolymers with a Broad Biomedical Potential

Dieter Michael Scheibel, Dandan Guo, Juntao Luo, and Ivan Gitsov*

Cite This: https://dx.doi.org/10.1021/acs.biomac.0c00126

Read Online



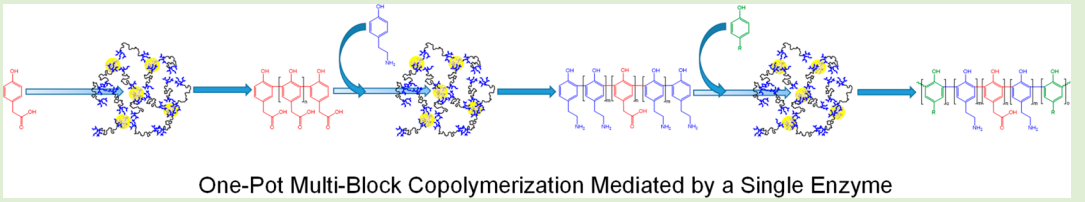

One-Pot Multi-Block Copolymerization Mediated by a Single Enzyme

**ABSTRACT:** This study describes a unique "quasi-living" block copolymerization method based on an initiation by a single enzyme. We use this term to describe a process where a preformed polymer chain can be reactivated to continue propagating with a second or third comonomer without addition of new catalyst. The presented strategy involves a laccase (oxidoreductase) mediated initial polymerization of 4-hydroxyphenylacetic acid to a homopolymer containing phenolic terminal units, which in turn can be easily reactivated by the same enzyme in the same reaction vessel to continue propagation with a second monomer (tyramine). Increased copolymer yield (up to 26.0%) and polymer molecular mass (up to $M_w$ = 116 000 Da) are achieved through the addition of previously developed micellar and hydrogel enzyme complexing agents. The produced poly(tyramine)-*b*-poly(4-hydroxyphenylacetic acid)-*b*-poly(tyramine) is water-soluble and able to self-assemble in aqueous solution. Both tyramine blocks were successfully modified with ibuprofen moieties (up to 24.6% w/w load) as an example for potential polymer drug conjugation. The copolymerization could be further extended with addition of a third (fluorescent) comonomer in the same reaction vessel to yield a fluorescent pentablock copolymer. The successful modifications and advantageous solution behavior of the produced copolymers demonstrate their viability as versatile drug delivery and/or bioimaging agents, as confirmed by cytotoxicity and cellular uptake studies.



## 1. INTRODUCTION

Development of "living" polymerization systems[1] has been of continuous interest to polymer chemists for the control in molecular mass and narrow dispersity they provide when compared with the conventional free radical- or condensation polymerization techniques. These advantages result from rapid and quantitative initiation, absence of side reactions, and extremely slow or absent chain termination processes.[2,3] "Living" polymerizations are also noteworthy for their ability to produce block copolymers which often display interesting self-assembly behavior[4] and have found numerous industrial uses including controlled drug delivery and release,[5−7] patterning in lithography,[8,9] and production of porous materials,[10−12] among many other applications. In contrast to conventional free radical polymerizations, which quickly undergo chain termination via radical coupling or disproportionation, this type of polymer synthesis can be utilized in the formation of block copolymers due to the significantly enhanced lifetime of the propagating active site owing to the absence of traditional bimolecular termination processes.[1,2]

Because of the inherent moisture sensitivity of true "living" anionic and cationic polymerizations, their incompatibility with numerous solvents (specifically protic solvents), and relatively limited monomer choice, recent work has focused on the development of pseudoliving polymerizations which aim to suppress chain termination rather than completely eliminate it. Such techniques include atom transfer radical polymerization (ATRP),[13,14] reversible addition−fragmentation chain transfer polymerization (RAFT),[15] and stable free radical mediated polymerization (SFRP).[16] Although these polymerization techniques have displayed good control of polymer molecular mass and dispersity in addition to being relatively robust, the occurrence of traditional chain termination and chain transfer reactions could cause some loss of functionality on the propagating polymer chain ends[17,18] and thus impede to a certain extent their applicability for the synthesis of block copolymers.

In addition to lack of byproducts and high stereo- and regiospecificity,[18−20] enzymes are often able to mediate

Received: January 27, 2020
Revised: April 1, 2020
Published: April 1, 2020

**Scheme 1. Oxidation Mechanism of Phenolic Substrates by Laccase and Phenoxy Radical Coupling Products**[a]

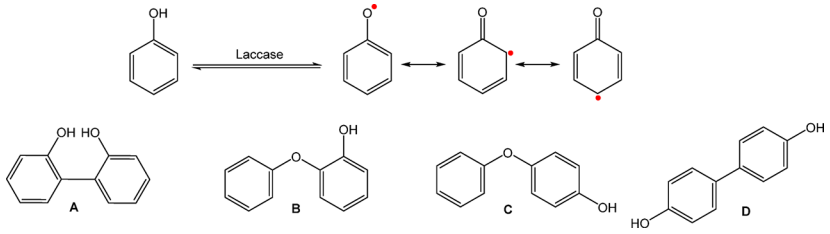


[a]Via C—C ortho coupling (A), C—O ortho coupling (B), C—O para coupling (C), and C—C para coupling (D).

polymerizations efficiently in either bulk or aqueous media at or near ambient temperatures,[21−23] minimizing solvent and energy expenditures. Of particular importance is their ability to induce different chemical transformations in a single-step procedure. Using these advantages, they have been tested as comonomer-specific initiators in chemo-enzymatic block copolymerizations.[24] This quoted paper reported the one-pot synthesis of poly(methyl methacrylate)-*b*-poly(ε-caprolactone) in supercritical $CO_2$ at 1500 psi using a bifunctional initiator, CuBr/bpy, and Novozym-435 as catalysts for the simultaneous ATRP polymerization of methyl methacrylate and lipase-mediated ring-opening polymerization of ε-caprolactone, respectively. Undoubtedly this strategy provides good options for the synthesis of block copolymers with unusual compositions; the use of specialized equipment and limited choice of monomers soluble in supercritical $CO_2$ being the major drawbacks. While our study was in progress, an enzymatic cascade reaction was reported for the construction of multiblock copolymers.[25] This interesting but rather elaborate strategy involves two enzymes: pyranose oxidase, which sole purpose is to produce $H_2O_2$ upon being fed with D-glucose, and a subsequently added horseradish peroxidase, which uses the peroxide to produce a radical from acetylacetone. This radical in turn triggers a reversible-deactivation radical polymerization and copolymerization of several water-soluble vinyl monomers in the presence of a chain transfer agent (a trithiocarbonate). Besides the addition of a comonomer, the synthesis of the block copolymers necessitates the addition of extra portions of the two enzymes, D-glucose and acetylacetone.[25]

In this current study, we report a new method of "quasi-living" environmentally benign one-pot block copolymerization mediated by a single enzyme without the use of any additional cocatalysts and reagents. Of the numerous enzymes capable of catalyzing polymerization, laccase, a benzenediol:oxygen oxidoreductase, has proven the ability to mediate the polymerization of numerous substrates including vinyl monomers and more commonly phenol and aniline derivatives.[26−28] The polymerization of phenolic substrates by this enzyme is known to occur via oxidation to a phenoxy radical with concomitant reduction of oxygen to water (Scheme 1).[29,30] The phenoxy radicals formed could undergo either C—C or C—O coupling at the ortho- or para- position, generating a polymer backbone composed of phenol and phenyl ether repeating units.

In contrast to previously mentioned controlled/living polymerization methods (i.e., ATRP, RAFT, and SFRP), laccase-mediated polymerizations of phenolic monomers do not undergo irreversible chain termination since the polymer chain formed could be reactivated (oxidized) even if the terminal phenoxy radical is quenched. The ability of laccase to reactivate and facilitate the continued propagation of the polymer chain was demonstrated in one of our previous articles where an increase in polymer molecular mass was observed upon the addition of a second portion of tyrosine monomer to a solution of preformed unnatural poly(tyrosine) and laccase.[31] This reactivation opens an intriguing "quasi-living" pathway to block copolymers by the simple addition of a second comonomer to the polymer chain upon depletion of the first substrate. To our knowledge, there is no analogue of this strategy in the published literature.

The proof of concept for this new method is demonstrated here by the copolymerization of two naturally derived comonomers: 4-hydroxyphenylacetic acid, 4HPAA, (frequently found in olive oil[32]) and 4-hydroxyphenylethylamine-tyramine, (common ingredient in plants[33]). The copolymerization yields poly(tyramine)-*b*-poly(4-hydroxyphenylacetic acid)-*b*-poly-(tyramine) being conducted in an aqueous buffer solution at pH 7 and 45 °C. It requires minimal reaction workup following an environmentally benign procedure. The molecular mass of the different blocks is controlled by changing the amount of comonomer feed.

## 2. EXPERIMENTAL SECTION

**2.1. Materials.** 4-Hydroxyphenylacetic acid, 4HPAA (99%), tyramine (99%), ±-2-(4-isobutylphenyl)propanoic acid (Ibuprofen, 99%), Rhodamine B Base (99%), anhydrous ethylene diamine (99%), *N*-(3-(dimethylamino)propyl)-*N*′-ethylcarbodiimide hydrochloride, EDC (98%), fluorescein (95%), 7-hydroxycoumarin (99%), pyrene (99%), 2,5-dihydroxybenzoic acid, DHB (99.5%) and laccase from *Trametes versicolor* (≥0.5 U/mg) (all from Sigma-Aldrich, St. Louis, MO), anhydrous methanol (99.9%, Alfa Aesar), ethyl acetate (99.5%, Spectrum Chemical), sulfuric acid (95−98%, J.T. Baker), maleic anhydride (99%, Sigma-Aldrich), dichloromethane, DCM (A.C.S. Reagent, J.T. Baker), sodium bicarbonate (99%, Alfa Aesar), and acetic anhydride (98%, J.T. Baker) were used as received. HPLC grade tetrahydrofuran, THF (from Pharmaco-Aaper, Oakland CA), was distilled prior to use, removing the inhibitor (butylated hydroxytoluene), which was found to retard laccase mediated polymerizations.

The synthesis of 2-(4-isobutylphenyl)-*N*-(2-aminoethyl)-propanamide maleimide (ibuprofen-EDA-maleimide) is described as follows (Scheme 2).

*Methyl 2-(4-isobutylphenyl)-N-(2-aminoethyl)propanoate (Ibuprofen Methyl Ester, 1).* To a 100 mL round-bottom flask connected to a water-cooled condenser was added ibuprofen (5.0 g, 0.024 mol), 50 mL of anhydrous methanol, and 1 mL of sulfuric acid. The solution was heated at reflux for 12 h after which the solution was dissolved in ethyl acetate and washed three times with deionized water. The solvent was removed by rotary evaporator and the product was obtained as a colorless oil. Yield: 4.91 g, 92%.

*$^1$H NMR (DMSO-$d_6$).* δ 7.24 (d, 2H), 7.05 (d, 2H), 3.78 (dd, 1H), 3.68 (s, 3H), 2.43 (d, 2H), 1.82 (m, 1H), 1. 61 (d, 3H), 0.91 (d, 6H).

*2-(4-Isobutylphenyl)-N-(2-aminoethyl)propanamide (Ibuprofen-EDA, 2).* To a 50 mL round-bottom flask connected to a water-cooled


https://dx.doi.org/10.1021/acs.biomac.0c00126
Biomacromolecules XXXX, XXX, XXX−XXX

**Scheme 2. Synthesis of Ibuprofen-EDA-Maleimide**

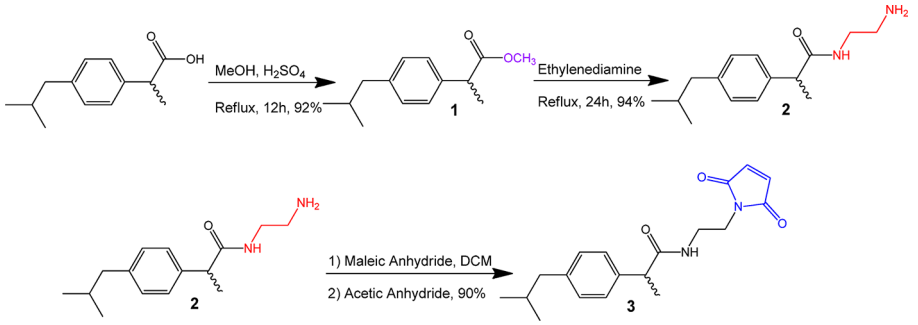


**Scheme 3. Synthesis of Fluorescent Monomer Fluor-EDA-HPAA**

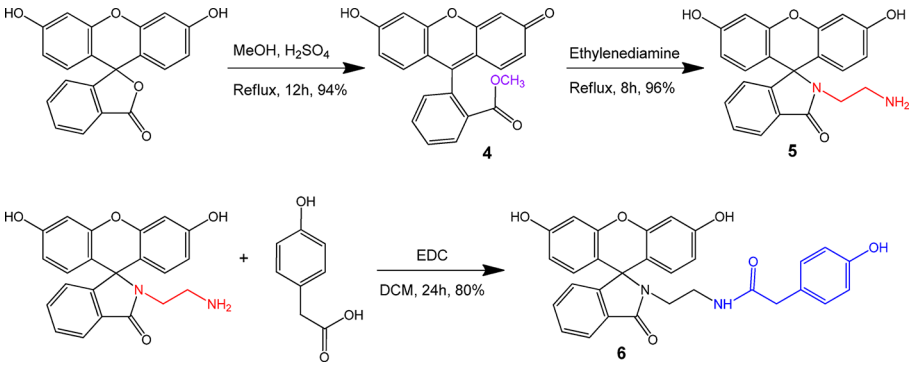


condenser was added **1** (4.9 g, 0.022 mol) followed by ethylene diamine (20 mL, 0.3 mol). The solution was heated at reflux for 24 h after which the solution was dissolved in ethyl acetate and washed three times with dilute sodium bicarbonate solution and finally with deionized water. The solvent was removed by rotary evaporator and product **2** was obtained as yellow oil. Yield: 4.71 g, 94%.

*$^1$H NMR (DMSO-$d_6$).* $\delta$ 8.03 (t, 1H), 7.25 (d, 2H), 7.03 (d, 2H), 5.18 (s, 2H), 3.48 (dd, 1H), 3.46 (t, 2H), 2.74 (t, 2H), 2.40 (d, 2H), 1.82 (m, 1H), 1.28 (d, 3H), 0.92 (d, 6H).

*2-(4-Isobutylphenyl)-N-(2-aminoethyl)propanamide Maleimide (Ibuprofen-EDA-Mal, **3**).* Ibuprofen-EDA (4.5 g, 0.018 mol), maleic anhydride (5.0 g, 0.05 mol), and dichloromethane (20 mL) were added to a 50 mL round-bottom flask, connected to a water-cooled condenser. The solution was stirred at room temperature for 24 h. After removing the solvent by rotary evaporation, acetic anhydride (10 mL, 0.09 mol) was added and the solution heated at reflux for 1 h after which an excess of water was slowly added to the solution. The aqueous solution was neutralized with sodium bicarbonate and the product was extracted with 50 mL portions of ethyl acetate. The removal of solvent by rotary evaporator afforded a solid off-white product. Yield: 5.35 g, 90%.

*$^1$H NMR (DMSO-$d_6$).* $\delta$ 8.0 (t, 1H), 7.3 (d, 2H), 7.08 (d, 2H), 6.96 (s, 2H), 3.49 (dd, 1H), 3.46 (t, 2H), 3.24 (t, 2H), 2.48 (d, 2H), 1.78 (m, 1H), 1. 31 (d, 3H), 0.83 (d, 6H). See also Figure 8.

The synthesis of fluorescein-labeled 4HPAA was accomplished using the following protocol, Scheme 3.

*Fluorescein Methyl Ester (Fluor-OMe, **4**).* Fluorescein (10.0 g, 0.030 mol), 50 mL of anhydrous methanol, and 5 mL of sulfuric acid were added to a 250 mL round-bottom flask connected to a water-cooled condenser. The solution was heated at reflux for 12 h after which the solution was neutralized with sodium bicarbonate and concentrated using a rotary evaporator. The residual solid was suspended in deionized water, mixed thoroughly, filtered, and washed with 200 mL deionized water. The product was dried overnight in a vacuum oven at 50 °C and obtained as a red solid. Yield: 9.82 g, 94%.

*$^1$H NMR (DMSO-$d_6$).* $\delta$ 8.15 (dd, 1H), 7.94 (td, 1H), 7.76 (td, 1H), 7.38 (dd, 1H), 7.29 (dd, 2H), 7.03 (d, 2H), 6.56 (dd, 2H), 3.56 (s, 3H).

*Fluorescein Ethylendiamine Spirolactam (Fluor-EDA, **5**).* Anhydrous ethylene diamine (50 mL) and **4** (5.0 g, 0.014 mol) were added to a 250 mL round-bottom flask connected to a water-cooled condenser. The solution was heated at reflux for 8 h. During that time, the solution color gradually changed from yellow to orange. The reaction mixture was concentrated to approximately 10 mL in volume and precipitated into deionized water. The precipitate was filtered, washed thoroughly with deionized water, and dried in a vacuum oven overnight at 50 °C producing a yellow solid. Yield: 5.17 g, 96%.

*$^1$H NMR (DMSO-$d_6$).* $\delta$ 7.78 (d, 1H), 7.51 (m, 2H), 6.99 (d, 1H), 6.60 (d, 2H), 6.45 (d, 2H), 6.39 (d, 2H), 2.97 (t, 2H), 2.17 (t, 2H).

*Fluorescein Ethylendiamine 4-Hydroxyphenylacetamide Spirolactam Derivative (Fluor-EDA-HPAA, **6**).* To a 100 mL round-bottom flask were added **5** (1.0 g, 0.027 mol), DCM (50 mL), EDC (6.2 g, 0.040 mol), and 4HPAA (6.2 g, 0.040 mol). The solution was allowed to stir for 24 h. The reaction solution was washed with three 20 mL portions of 0.5 M HCl, three 20 mL portions of sodium bicarbonate solution, and finally with deionized water until a neutral pH was attained. The organic layer was dried over anhydrous sodium sulfate, decanted, and solvent evaporated via rotary evaporator to yield a yellow solid. Yield: 1.09 g, 80%.

*$^1$H NMR (DMSO-$d_6$).* $\delta$ 9.49 (br), 7.81 (t, 1H), 7.51 (m, 2H), 6.99 (d, 1H), 6.93 (d, 2H), 6.62 (d, 2H), 6.58 (d, 2H), 6.58 (d, 2H), 6.45 (d, 2H), 6.39 (d, 2H), 3.11 (s, 2H), 3.03 (t, 2H), 2.76 (q, 2H).

The synthesis of Rhodamine-labeled 4HPAA was accomplished as follows (Scheme 4).

*Rhodamine B Ethylenediamine Spirolactam (Rhd-EDA, **7**).* To a 100 mL round-bottom flask was added Rhodamine B Base (5.0 g, 0.011 mol) and 50 mL of anhydrous ethylenediamine. The solution was heated at reflux for 24 h. The solvent was then removed via rotary evaporator and the residual solid suspended in deionized water. The suspension was filtered and washed with deionized water until a colorless filtrate was obtained. It was dried overnight in a vacuum oven at 50°°C yielding a pink solid. Yield: 5.20 g, 95%.

*$^1$H NMR (DMSO-$d_6$).* $\delta$ 7.77 (d, 1H), 7.49 (m, 2H), 6.99 (m, 1H), 6.35 (m, 6H), 3.33 (q, 8H), 2.97 (t, 2H), 2.19 (t, 2H), 1.09 (t, 12H).

*Rhodamine B Ethylenediamine 4-Hydroxphenylacetamide Spirolactam Derivative (Rhd-EDA-HPAA, **8**).* 4HPAA (4.65 g, 0.030


https://dx.doi.org/10.1021/acs.biomac.0c00126
Biomacromolecules XXXX, XXX, XXX−XXX

**Scheme 4. Synthesis of Fluorescent Monomer Rhd-EDA-HPAA**

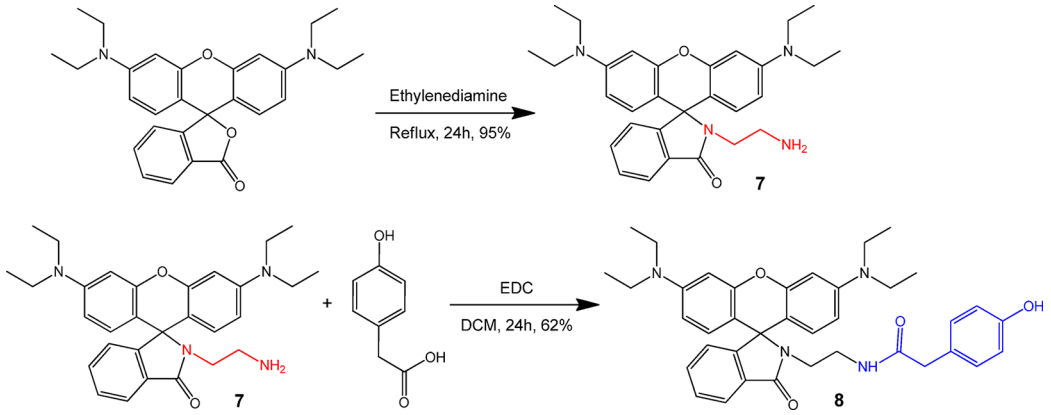


mol), 50 mL DCM, EDC (4.65 g, 0.030 mol), and **7** (1.0 g, 0.021 mol) were added to a 100 mL round-bottom flask. The solution was allowed to stir at room temperature for 24 h. The reaction mixture was washed with three 20 mL portions of 0.05 M HCl, three 20 mL portions of sodium bicarbonate solution, and finally with deionized water until a neutral pH was achieved. The organic layer was dried over anhydrous sodium sulfate, decanted, and solvent evaporated in rotary evaporator to yield a pink solid. Yield: 0.79 g, 62%.

*$^1$H NMR (DMSO-$d_6$).* $\delta$ 9.21 (s, 1H), 7.80 (s, 1H), 7.52 (m, 3H), 6.97 (s, 1H), 6.93 (d, 2H), 6.60 (d, 2H), 6.35 (m, 6H), 3.30 (q, 8H), 3.10 (s, 2H), 3.05 (t, 2H), 2.79 (q, 2H), 1.06 (t, 12H).

Linear$_{(A)}$−linear$_{(B)}$ and linear−hyperbranched complexing agents composed of poly(ethylene glycol), PEG, and either poly(styrene), PS, or poly(*p*-chloromethylstyrene), PPCMS, were synthesized by atom transfer radical polymerization of either styrene or *p*-chloromethylstyrene initiated by $\alpha$-chlorophenylacetyl capped poly(ethylene glycol).[34] Their designations are PPCMS2.3k-13k-PPCMS2.3k and PS4.2k-PEG20k-PS4.2k, where the numbers reflect the molecular mass of the corresponding block (PPCMS, PEG, and PS).

**2.2. Instrumentation and Methods.** *2.2.1. Chromatography.* Size exclusion chromatography (SEC) was conducted on a system consisting of a Waters 1515 isocratic pump, a Waters 1500 series manual injector, two PolyPore 5 $\mu$m 300 mm × 7.5 mm mixed bed columns (Polymer Laboratories, Ltd.), and a Waters 2414 refractive index detector. All analyses were conducted at 60 °C with dimethyl sulfoxide (DMSO) as eluent containing 0.1% (1 mg/mL) LiBr at a flow rate of 0.8 mL/min. Sample solutions were filtered using a 0.45 $\mu$m cellulose acetate filters prior to injection. Calibration was performed using 15 monodisperse poly(ethylene glycol) and poly(ethylene oxide) standards (1.98−452 kDa). Molecular mass calculations were accomplished with Waters Breeze 3.3 software.

*2.2.2. NMR Spectroscopy.* $^1$H NMR and $^{13}$C NMR spectra were recorded using HCl-doped DMSO-$d_6$ as solvent at 22 °C on a Bruker AVANCE 600 MHz instrument with the solvent signal as the internal standard.

*2.2.3. Fluorescence Spectroscopy.* All fluorescence measurements were performed on a Horiba Fluorolog-3 spectrophotometer with a SpectrAcq system controller. The instrument used a xenon arc lamp source. Fluorescence measurements were conducted at 90° using an excitation wavelength of 490 nm for fluorescein derivatives or 334 nm for pyrene in water. Quantum yield of polymer samples were calculated using fluorescein and 7-hydroxycoumarin (umbelliferone) as standards.

*2.2.4. UV−vis Spectroscopy.* All UV−vis spectroscopic measurements were conducted on an Agilent 8453 UV−vis spectrophotometer at room temperature in deionized water unless otherwise specified.

*2.2.5. FT-IR ATR Spectroscopy.* Fourier transform infrared spectroscopy (FT-IR ATR) spectra were obtained on a Bruker Tensor 27 spectrophotometer with a MIR source and a DLaTGS detector. Spectra were recorded under ambient conditions at a resolution of 4 cm$^{-1}$. A total of 64 scans were recorded for each spectrum in addition to the background.

*2.2.6. Dynamic Light Scattering (DLS).* All DLS measurements were performed on a Malvern Zetasizer ZS instrument. The instrument used a 633 nm laser source with a fixed backscattering detector at 173°. Size calculations were performed using a CONTIN procedure.

*2.2.7. Thermogravimetric Analysis (TGA).* TGA measurements were conducted on a TGA Q5000IR (TA Instruments). A temperature ramp of 10 °C/min was used from room temperature to 700 °C under a nitrogen flow (10 mL/min).

*2.2.8. Matrix-Assisted Desorption and Ionization Time-of-Flight Analysis (MALDI-TOF).* MALDI-TOF MS spectra were collected on a Bruker Autoflex III having Smartbeam II laser source (Nd:YAG laser, 266 or 355 nm). Spectra were acquired in linear positive mode with the attenuation set to the lowest value capable of obtaining high-resolution spectra. A matrix solution was formed by dissolving DHB in deionized water (18.1 MΩ) at a concentration of 80 mg/mL. Sample solutions were prepared in deionized water (18.1 MΩ) at a concentration of 1 mg/mL. Samples were spotted by mixing matrix solution and sample solution in a 1:1 ratio and spotting 5 $\mu$L of the resulting solution on a MTP 384 target plate (polished steel, Bruker Daltronics).

*2.2.9. Determination of Critical Aggregation Concentration.* Critical aggregation concentration (CAC) was determined using two methods. CAC was first determined using pyrene as a fluorescent probe and was conducted by making polymer solutions of various concentrations in deionized water and adjusting their pH to 7 with dilute HCl and NaOH. Five microliters of 0.1 mM pyrene in ethanol was then added. After a 30 min incubation period, the fluorescence spectra of the solutions were recorded from 360 to 500 nm using an excitation wavelength of 334 nm and slit width of 1 nm. The ratio of peak intensity at 384 to 373 nm was plotted against concentration and the lower inflection point designated as the CAC.

CAC of the synthesized copolymers was verified using DLS and measuring hydrodynamic diameter. Polymer solutions of similar concentrations as above were made in deionized water and similarly adjusted to pH 7 with dilute HCl and NaOH. The hydrodynamic diameter of the polymer solutions was plotted against concentration, and the lower inflection point in the curve was used to estimate the CAC.

**2.3. Syntheses.** *2.3.1. Block Copolymerization of 4-Hydroxyphenylacetic Acid and Tyramine.* A typical copolymerization was conducted by first preparing a 0.2 M pH 7 potassium phosphate buffer. To 200 mL of buffer solution, 200 mg of laccase is added. In some cases, 200 mg of complexing agent, dissolved in 2 mL of distilled THF, was added dropwise under vigorous stirring. The solution was allowed to acclimate for 4 h at 45 °C. 4HPAA (600 mg, 3.95 mmol) was supplemented under stirring. The polymerization was allowed to proceed for 72 h at 45 °C after which the polymerization mixture was divided into 20 mL portions. An aliquot was taken to


https://dx.doi.org/10.1021/acs.biomac.0c00126
Biomacromolecules XXXX, XXX, XXX−XXX

**Table 1. Effect of Comonomer Feed on Copolymer Molecular Mass and Yield**

| entry[a] | 4HPAA (mg) | Tyramine (mg) | $M_w$[b] | $M_p$[c] | $M_n$[b] | $M_n$[d] | $Đ$[e] | yield (%) |
|---|---|---|---|---|---|---|---|---|
| N1 | 60 | 0 | 12700 | 7000 | 7500 | | 1.70 | 97.0 |
| N2 | 60 | 5 | 116000 | 23500 | 41000 | 7300 | 2.83 | 87.5 |
| N3 | 60 | 10 | 95500 | 22000 | 35700 | 8300 | 2.67 | 79.4 |
| N4 | 60 | 15 | 51500 | 19900 | 24200 | 8700 | 2.13 | 75.6 |
| N5 | 60 | 20 | 27800 | 16500 | 16500 | 9300 | 1.68 | 70.2 |
| N6 | 60 | 25 | 29000 | 15400 | 15800 | 9400 | 1.82 | 67.7 |
| N7 | 60 | 30 | 25500 | 14900 | 15000 | 10000 | 1.70 | 62.8 |
| N8 | 60 | 35 | 26800 | 10700 | 13200 | 10500 | 1.92 | 59.7 |
| N9 | 60 | 40 | 24500 | 9400 | 11700 | 10700 | 2.08 | 58.4 |

[a]Native laccase used as biocatalyst without complexing agents. [b]Calculated via SEC using PEG standards. [c]Molecular mass at the peak apex in the SEC traces. [d]Calculated via $^1$H NMR spectroscopy assuming $M_n$ = 7500 for entry N1 and using it as the reference value to compare the integral intensity ratio between the $H_d$ protons in poly(4-HPAA) and $H_f$ + $H_e$ protons in the poly(tyramine) block, see Figure 4. [e](Co)polymer dispersity ($M_w/M_n$)

**Scheme 5. Synthesis and Post-Polymerization Modification of Poly(tyramine)-*b*-poly(4HPAA)-*b*-poly(tyramine)[a]**

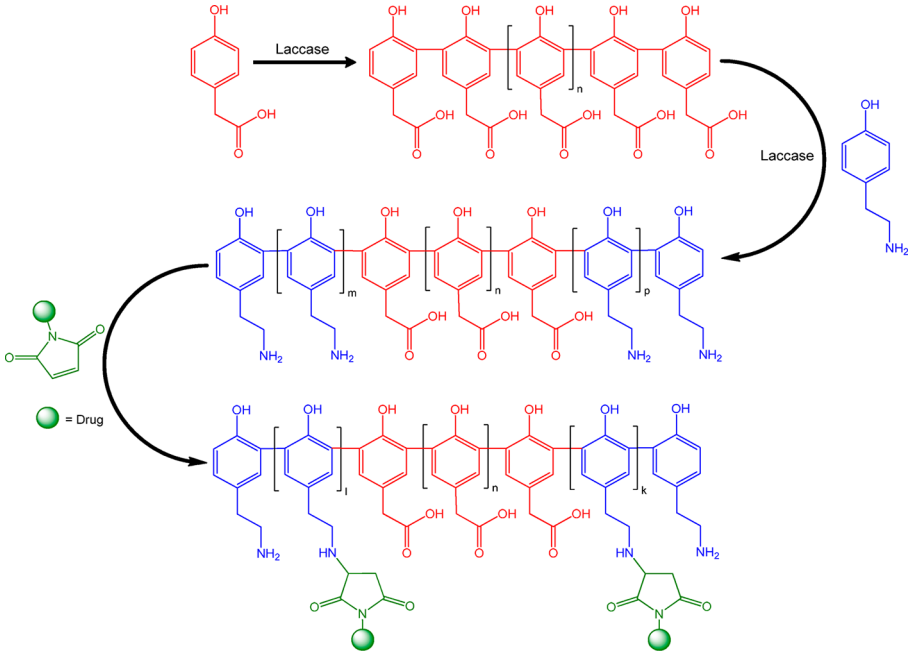


[a]Only the C—C coupling adducts are shown for simplicity.

serve as a reference for the molecular mass of the initial block (molecular mass was determined via SEC using PEG standards). A predetermined amount of tyramine was then added to each 20 mL portion and the copolymerization was allowed to proceed for an additional 72 h at 45 °C. Polymer isolation was conducted by initially precipitating the copolymer via acidification of the solution to a pH < 2. The precipitate was collected via centrifugation and washed three times with 0.2 M HCl and last with deionized water. The acidic washes served to remove unreacted monomer, biocatalyst, and any homo poly(tyramine) produced. MALDI-TOF and SEC analysis of the supernatant revealed that residual material was primarily unreacted tyramine monomer with little to no poly(tyramine) formed (Figure S16). In some cases, the sediment was washed with THF to remove complexing agent. Polymer yield was calculated from the ratio of the isolated and purified product to the initial amounts of comonomers added (see Table 1).

*2.3.2. Block Copolymerization of 4HPAA and Fluorescein or Rhodamine Derivatives.* Block copolymerizations of 4HPAA with Fluor-EDA-HPAA and Rhd-EDA-HPAA were conducted by adding 60 mg of preformed poly(4-HPAA) to 20 mL of an equilibrated solution of buffered enzyme or enzyme-complex solution at 45 °C (preparation described in Section 2.3.1). Twenty milligrams of either Fluor-EDA-HPAA or Rhd-EDA-HPAA comonomer was then immediately added to the polymerization vessel and the reaction was allowed to proceed for 72 h. Reaction workup was performed as described in Section 2.3.1. To remove unreacted comonomer, additional washes with THF were conducted.

*2.3.3. Random Copolymerization of 4HPAA and Tyramine.* Random copolymerizations of 4HPAA and tyramine were conducted using a similar procedure as described in Section 2.3.1; however, both monomers were added in one portion and the reaction halted after 72 h.

*2.3.4. Postpolymerization Modification of Poly(tyramine)-b-poly(4HPAA)-b-poly(tyramine).* Conjugation of ibuprofen-EDA-maleimide to poly(tyramine)-*b*-poly(4HPAA)-*b*-poly(tyramine) was conducted immediately after the incorporation of the poly(tyramine) blocks via Aza-Michael addition of the ibuprofen-EDA-maleimide to the primary amines of the tyramine repeating units in the same copolymerization flask. The reaction was conducted at 45 °C for 72 h. Purification of the modified copolymer was accomplished as described in Section 2.3.1. $^1$H NMR was used to quantify ibuprofen attachment to the block copolymer.

*2.3.5. Cell Viability and Cellular Uptake Studies.* See Supporting Information for a detailed description


https://dx.doi.org/10.1021/acs.biomac.0c00126
Biomacromolecules XXXX, XXX, XXX−XXX

## 3. RESULTS AND DISCUSSION

**3.1. Synthesis of Poly(tyramine)-*b*-poly(4HPAA)-*b*-poly(tyramine).** In this study, block copolymers composed

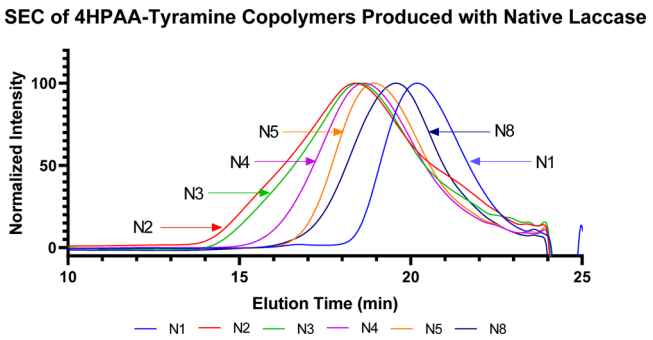


**Figure 1.** SEC elution curves of 4HPAA−tyramine block copolymers with 0.1% LiBr in DMSO as eluent. See Table 1 for sample designations. See also Figure S1 showing SEC traces of all copolymers.

of tyramine and 4HPAA were enzymatically synthesized by laccase, using a unique quasi-living polymerization procedure. The interior 4HPAA block was first made by the enzyme-mediated homopolymerization of 4HPAA. After 72 h, the exterior polymer blocks were formed by addition of tyramine to the homopolymer solution in the original reaction vessel still containing the initial amount of catalytically active laccase, Scheme 5.

The synthesis of the ABA block copolymers containing A blocks with different molecular masses was monitored by SEC (Figures 1, S1, S2, and S3) and $^1$H NMR spectroscopy. The copolymers appeared as monomodal peaks in the SEC traces but interestingly had decreasing hydrodynamic volumes with the increase of comonomer feed (Figure 1). A similar trend was observed with the DLS analyses of the same samples (Figure 2).

This seemingly strange behavior could be explained by the occurrence of intramolecular interactions between the central 4HPAA B block and segments from the poly(tyramine) A blocks. At low tyramine feed, those A blocks were short and could not prevent the copolymer random coils of expanding in the SEC eluent (Figures 1 and 2, N2). When the feed increased, A blocks increased in length and the amino groups in their repeating units were able to interact with the carboxylic

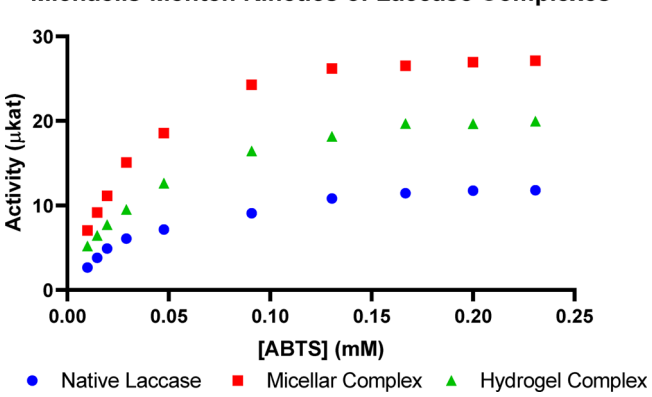


**Figure 3.** Michaelis−Menten kinetics of native laccase (blue circles), micelle−laccase complex with PPCMS2.3k-PEG13k-PPCMS2.3k (red squares), and hydrogel−laccase complex with PS2.4k-PEG13k-PS2.4k (green triangles). Deionized water, pH 7, room temperature.

**Table 2. Effect of Complexing Agent on Maximum Enzyme Activity and Substrate Binding**

| complex | $K_m$ (mM) | $V_{max}$ ($\mu$kat) |
|---|---|---|
| native | 0.04 | 14.2 |
| micelle[a] | 0.035 | 32.7 |
| hydrogel[b] | 0.03 | 22.1 |

[a]PPCMS2.3k-PEG13k-PPCMS2.3k used as complexing agent. [b]PS4.2k-PEG20k-PS4.2k used as complexing agent.

groups in the repeating units of the central B block (Figures 1 and 2, N3−9). The extensive hydrogen bonding and electrostatic interaction would then shrink the copolymer coils in the solutions. This assumption would be proven correct if a molecular mass analysis could be performed with a technique that does not depend on the hydrodynamic volume of the copolymers. Indeed, $M_n$ values of the same copolymers calculated by $^1$H NMR showed a clear growth tendency with the increase of the tyramine comonomer concentration, Table 1. A notable exception is only N2, where part of the initial central block remained unreacted (Figures 1 and 2, N1−N2).

In our previous study,[34] we found that the addition of micellar and hydrogel complexing agents to the reaction system increases enzyme activity and polymer yields. Here, we were using two typical representatives of these complexing

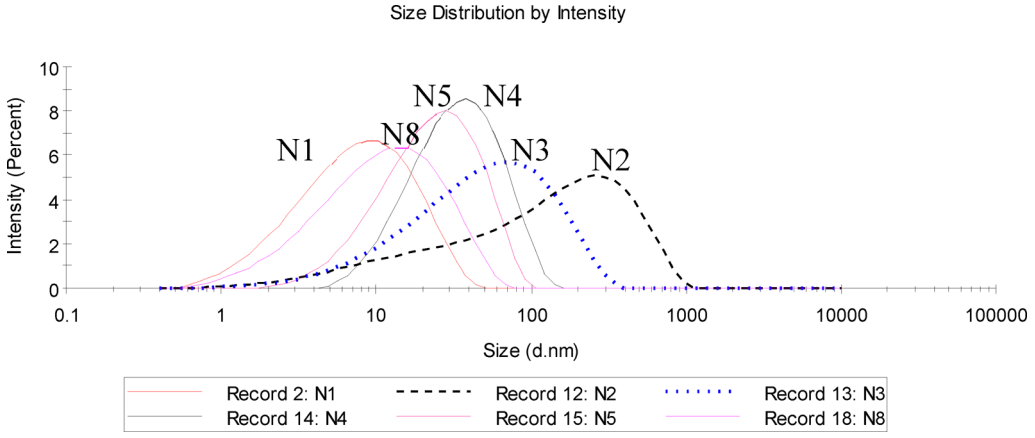


**Figure 2.** Hydrodynamic diameters of 4HPAA−tyramine copolymer solutions in DMSO below CAC.


https://dx.doi.org/10.1021/acs.biomac.0c00126
Biomacromolecules XXXX, XXX, XXX−XXX

**Table 3. Effect of Complexing Agent on Copolymer Molecular Mass and Yield**

| entry | complexing agent | 4HPAA (mg) | tyramine (mg) | $M_w$[a] | $M_p$[a] | $M_n$[a] | $M_n$[b] | $Đ$[a] | yield (%) |
|---|---|---|---|---|---|---|---|---|---|
| N7[c] | native | 60 | 30 | 25500 | 14900 | 15000 | 10000 | 1.70 | 62.8 |
| M7[d] | micelle[f] | 60 | 30 | 21700 | 12000 | 13900 | 10200 | 1.55 | 67.9 |
| H7[e] | hydrogel[g] | 60 | 30 | 17700 | 8400 | 10800 | 10900 | 1.64 | 88.8 |

[a]Calculated via SEC using PEG standards. [b]Calculated via $^1$H NMR spectroscopy with respect to the $M_n$ of the 4HPAA homopolymer. [c]Entry N7 from Table 1. [d]Entry M7 from Table S1. [e]Entry H7 from Table S2. [f]PPCMS2.3k-PEG13k-PPCMS2.3k used as complexing agent. [g]PS4.2k-PEG20k-PS4.2k used as complexing agent.

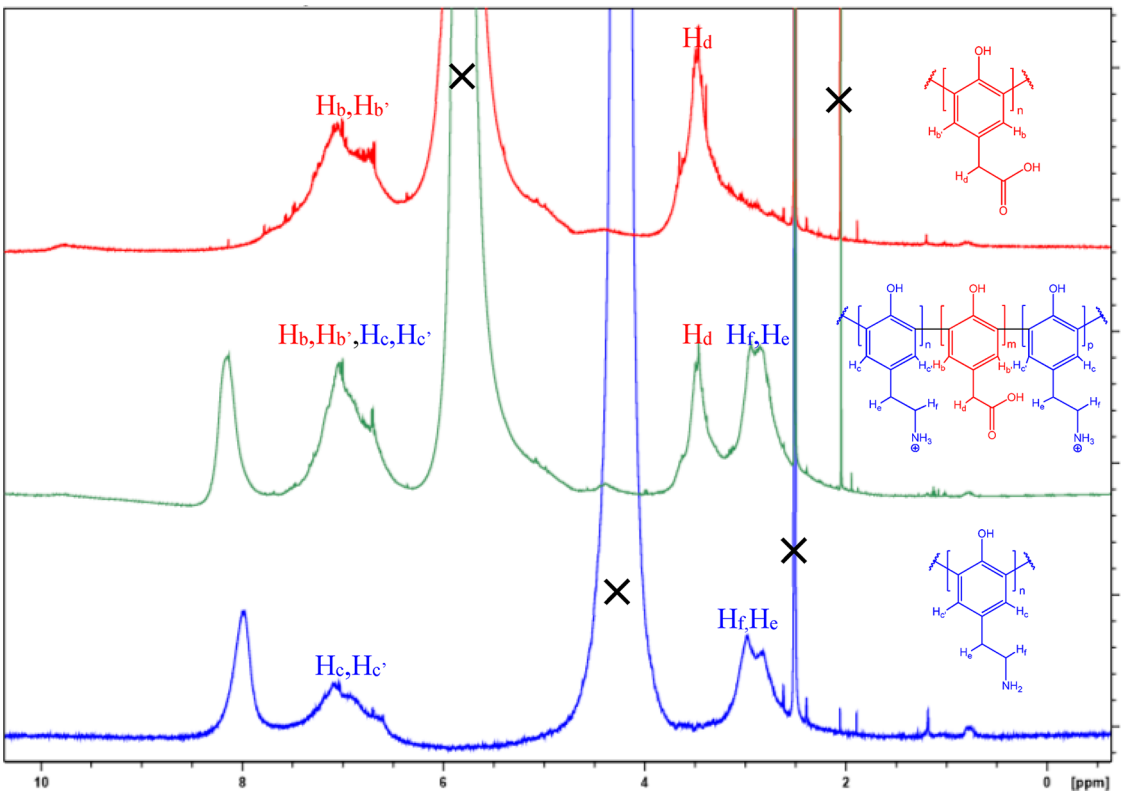


**Figure 4.** $^1$H NMR spectra (600 MHz) of poly(4-HPAA) (red), poly(tyramine)-*b*-poly(4-hydroxyphenylacetic acid)-*b*-poly(tyramine) (green), and poly(tyramine) (blue) recorded at 22 °C in DMSO-$d_6$/HCl. Solvent impurities are marked with (×).

agents, PPCMS2.3k-PEG13k-PPCMS2.3k (micelle forming) and PS4.2k-PEG20k-PS4.2k (hydrogel forming). The effect these complexing agents had on both maximal enzyme activity ($V_{max}$) and the efficiency of substrate binding to the enzyme complex ($K_m$) was determined as previously described[34] using 2,2′-azino-bis(3-ethylbenzothiazoline-6-sulfonic acid and Lineweaver−Burk plot (see Figure S18), Figure 3 and Table 2.

The yield of the 4HPAA−tyramine block copolymers was positively affected and increased by up to 9.4% (micelle) and 26.0% (hydrogel), Table 3. As the yield and molecular mass of the interior poly(4-hydroxyphenylacetic acid) block was not significantly affected by the addition of complexing agents (Tables 1, S1, and S2), the improved copolymer yield could be attributed to the formation of the poly(tyramine) blocks. This buildup was enabled by the enzyme complexes' ability to actively sequester the tyramine comonomer, which was only slightly soluble in the aqueous polymerization medium. This low comonomer solubility explains the decrease in copolymer yields observed when only native laccase was used, Table 1. With the amphiphilic complexing agents, the tyramine concentration around the enzyme active site was increased, facilitating generation of the active tyramine phenoxy radicals and enhancing copolymerization rate. As 4HPAA was inherently highly water-soluble, enabling ample interaction with the native laccase, it was not surprising that addition of complexing agents had a minimal effect on polymerization yield or poly(4HPAA) molecular mass, Tables 1, S1, and S2.

**3.2. Characterization of Poly(tyramine)-*b*-poly(4HPAA)-*b*-poly(tyramine).** Characterizations of poly(tyramine)-*b*-poly(4HPAA)-*b*-poly(tyramine) copolymers synthesized using either native laccase or laccase complexes were conducted using NMR and FT-IR ATR spectroscopy. $^1$H NMR spectra of the produced block copolymers (Figure 4) displayed broad peaks characteristic of the rigid phenyl backbone. Signals from 8.5 to 7.75 ppm were assigned to protons of the pronated amine of the tyramine repeat unit. Aromatic protons $H_b$, $H_{b''}$, $H_c$, $H_{c'}$ were visible within 7.5−6.5 ppm. Benzylic protons of the poly(4-hydroxyphenylacetic acid) interior block $H_d$ were assigned to the signals from 3.75 to 3.25 ppm, while the signals in the region of 3.25−2.5 ppm were attributed to the ethylene protons $H_e$ and $H_f$ of the poly(tyramine) blocks. The $^{13}$C NMR and FT-IR ATR spectra of the synthesized block copolymers are provided in the Supporting Information (Figures S6 and S7).

TGA of poly(tyramine)-*b*-poly(4HPAA)-*b*-poly(tyramine), Figure 5 green trace, displays two distinct decomposition


https://dx.doi.org/10.1021/acs.biomac.0c00126
Biomacromolecules XXXX, XXX, XXX−XXX

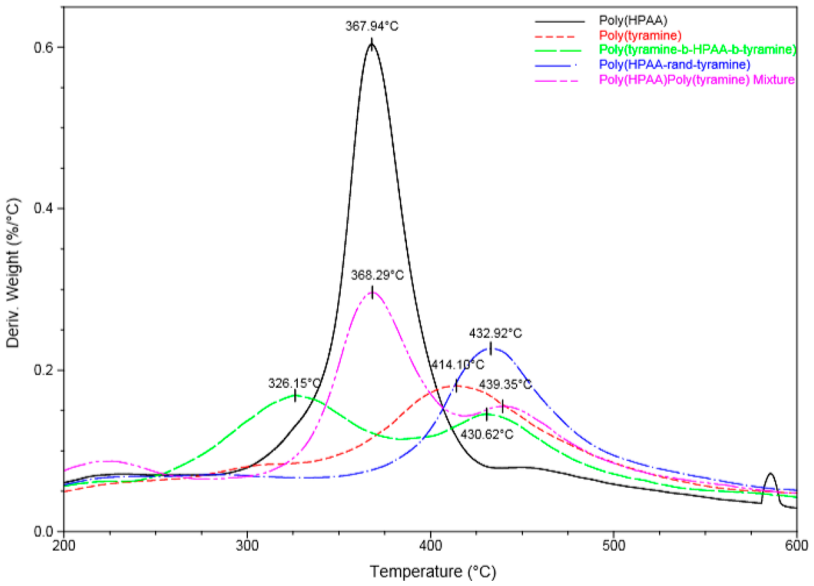


**Figure 5.** Differential TGA thermogram of poly(4HPAA), black; poly(tyramine), red; poly(tyramine)-*b*-poly(4HPAA)-*b*-poly(tyramine), green; random poly(tyramine-*co*-4HPAA), blue; and a mixture of poly(4-HPAA) and poly(tyramine), pink. TGA thermograms of monomers and the mixture of homopolymers are provided in the SI.

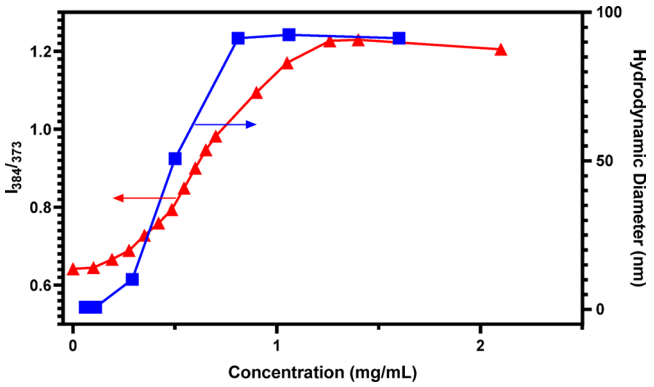


**Figure 6.** Fluorescence intensity ratios of pyrene excitation bands ($I_{384}/I_{373}$) depending on the concentration of poly(tyramine)-*b*-poly(4HPAA)-*b*-poly(tyramine), Table 1, N7: orange triangles. Hydrodynamic diameter of poly(tyramine)-*b*-poly(4HPAA)-*b*-poly(tyramine) depending on concentration measured by dynamic light scattering at pH 7, Table 1, N7: blue squares.

stages at 326.15 and 430.62 °C corresponding to degradation of the carboxylic groups in the 4HPAA block and the amine functionalities in the tyramine repeating units, respectively. Similar decomposition events are observed for the homopolymers poly(4HPAA) and poly(tyramine) at 367.94 and 414.10 °C (Figure 5, black and red traces). Differences in degradation events between the block copolymer and the homopolymers are attributed to the zwitterionic nature of the block copolymer resulting in the presence of a carboxylate anion of decreased stability compared to the free acid of the homopolymer. Similarly, the protonated amine of the block copolymer provides increased stability resulting in a higher degradation temperature. The decomposition pattern is notably different from the decomposition behavior of the random copolymer, which showed a single decomposition event at 432.92 °C. Increased thermal stability of the random copolymer may be due to intermolecular hydrogen bonding of the side chains stabilizing the carboxylic and amine functional groups. These TGA analyses provide an additional independent proof that a block copolymer formation is strongly favored over the homopolymerization of the tyramine added.

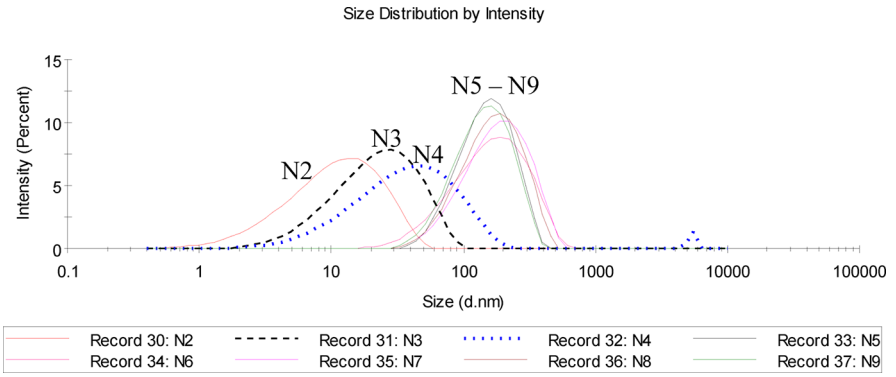


**Figure 7.** Hydrodynamic diameter of 4HPAA−tyramine copolymer micelles at a concentration of 1 mg/mL (above CAC) formed in pH 7 buffer solution (Table 1, N2−N9).


https://dx.doi.org/10.1021/acs.biomac.0c00126
Biomacromolecules XXXX, XXX, XXX−XXX

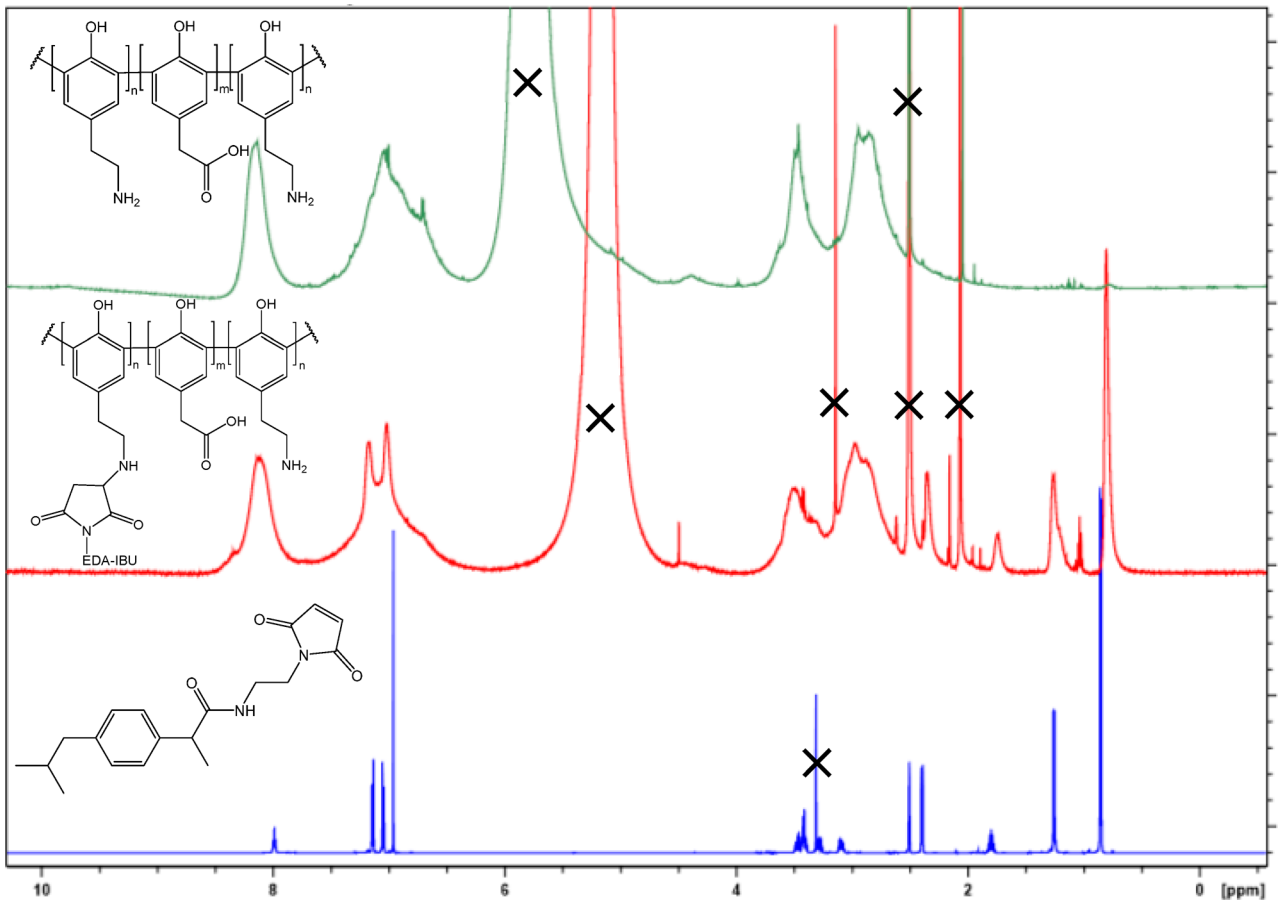


**Figure 8.** $^{1}$H NMR spectra (600 MHz) of poly(tyramine)-*b*-poly(4HPAA)-*b*-poly(tyramine), top green; ibuprofen conjugated poly(tyramine)-*b*-poly(4HPAA)-*b*-poly(tyramine), middle red; and ibuprofen-EDA-maleimide (bottom, blue). Solvent impurities are marked with (×).

**Table 4. Effect of Complexing Agent on Ibuprofen-EDA-Maleimide Addition to Poly(tyramine)-*b*-poly(4HPAA)-*b*-poly(tyramine)[a]**

| entry | complexing agent | 4HPAA (mg) | tyramine (mg) | ibuprofen incorporated (wt %)[a] |
|---|---|---|---|---|
| N7-I | native | 60 | 30 | 24.6 |
| M7-I | micelle[b] | 60 | 30 | 14.1 |
| H7-I | hydrogel[c] | 60 | 30 | 18.0 |

[a]An equimolar amount of ibuprofen-EDA-maleimide relative to tyramine was added in the same reaction flask immediately after the copolymerization of the tyramine block. [b]Calculated by $^{1}$H NMR spectroscopy. [c]PPCMS2.3k-PEG13k-PPCMS2.3k used as complexing agent. [d]PS4.2k-PEG20k-PS4.2k used as complexing agent.

**3.3. Critical Aggregation Concentration Determination of Poly(tyramine)-*b*-poly(4HPAA)-*b*-poly(tyramine).** The addition of two blocks of limited water solubility provides interesting application possibilities based on the characteristic amphiphilic character of these block copolymers. Critical aggregation concentration was determined by monitoring changes in the fluorescence spectra of pyrene.[35] This change in fluorescence was quantified by measuring the fluorescence intensity ratio at 384−373 nm (Figure 6, red triangles). The onset of aggregation was determined by the intersection of the regions of the low and sharp rise in the ratio of the two intensities and was found to be 0.25 mg/mL.

This result was verified by measuring the hydrodynamic diameter of the same copolymer at various concentrations by dynamic light scattering (Figure 6, blue squares), where onset micellization concentration of 0.21 mg/mL was determined. The broad concentration range over which an increase in fluorescence intensity ratio and hydrodynamic diameter is observed may be attributed to the relatively disperse copolymer. Notably the random copolymer did not change its hydrodynamic diameter with an increase in concentration (Figure S10), providing another independent proof that the sequential addition of a second comonomer to the preformed poly(4-HPAA) steered the process toward a block copolymer formation.

All copolymers self-assemble at concentrations close to 1 mg/mL, Figure 7. It should be noted that in contrast to the decreasing sizes at concentrations below CAC (Figure 2), the hydrodynamic diameters of the copolymer aggregates above CAC grow with increased molecular mass of the hydrophobic poly(tyramine) blocks (Figure 7, N3−N9). The practical size overlap observed with N6−N9 could be attributed to the increased entanglement and collapse of the aggregate core with the enlarged poly(tyramine) blocks.

These results also hint at the mechanism of propagation for these comonomers. Both have three reactive sites: the two ortho-positions in the benzene ring and the phenolic hydroxyl group. Therefore, a potential three-dimensional growth involving all possible sites could lead to loosely branched or even hyperbranched macromolecules. However, such structures would not undergo such a dramatic size change above CAC due to their increasingly rigid structures. That is why we


https://dx.doi.org/10.1021/acs.biomac.0c00126
Biomacromolecules XXXX, XXX, XXX−XXX

**Scheme 6. Block Copolymerization of Fluorescent Comonomers**[a]

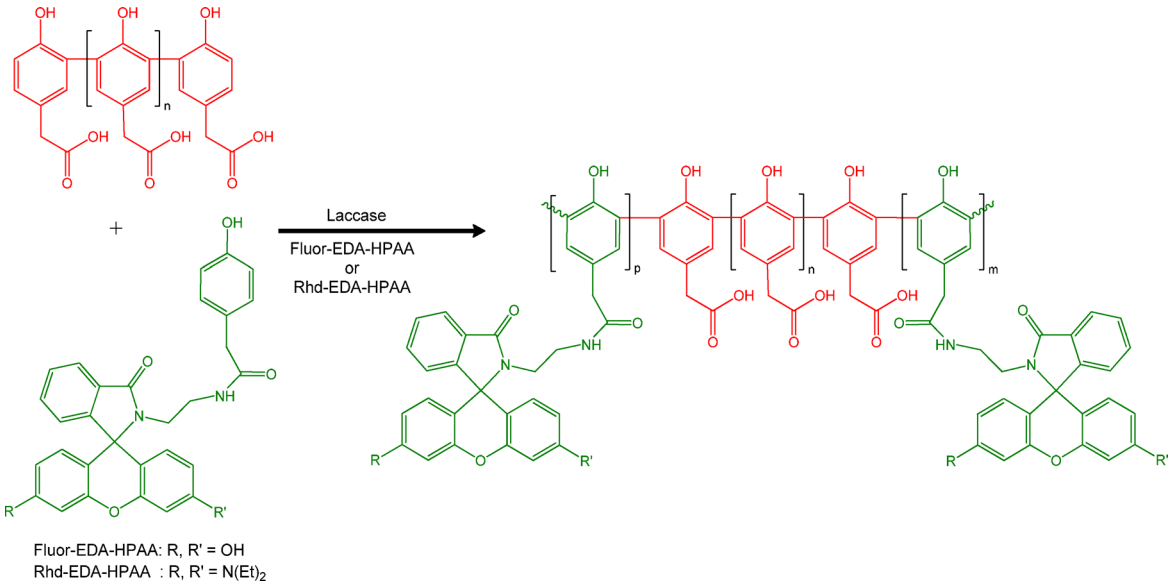


[a]Only C—C linkages shown.

**Table 5. Effect of Complexing Agent on Fluorescein Comonomer Addition to Poly(4HPAA)**[a]

| entry | complexing agent | poly(4HPAA) feed (mg) | Fluor-EDA-HPAA feed (mg) | Fluor-EDA-HPAA incorporated (wt %)[b] | quantum yield |
|---|---|---|---|---|---|
| N-FEH | native | 60 | 20 | 5.7 | 0.07 |
| M-FEH | micelle[c] | 60 | 20 | 11.3 | 0.15 |
| H-FEH | hydrogel[d] | 60 | 20 | 9.9 | 0.13 |

[a]Reaction conditions described in Section 2.3.1. [b]Calculated via UV−vis spectroscopy. [c]PPCMS2.3k-PEG13k-PPCMS2.3k used as complexing agent. [d]PS4.2k-PEG20k-PS4.2k used as complexing agent.

**Table 6. Molecular Mass Effects of Complexing Agent on Fluorescein Comonomer Addition to Poly(4HPAA)**[a]

| entry | complexing agent | $M_n$ | $M_w$ | $M_p$ | $Đ$ |
|---|---|---|---|---|---|
| poly(4-HPAA) | | 8200 | 16800 | 8500 | 2.05 |
| N-FEH | native | 9600 | 18900 | 8800 | 1.97 |
| M-FEH | micelle[b] | 12300 | 22200 | 11600[d] | 1.81 |
| H-FEH | hydrogel[c] | 9800 | 19600 | 10700 | 2.01 |

[a]Reaction conditions described in Section 2.3.1. [b]PPCMS2.3k-PEG13k-PPCMS2.3k used as complexing agent. [c]PS4.2k-PEG20k-PS4.2k used as complexing agent. [d]Corresponding to addition of six monomer units

**Table 8. MM Effect of Complexing Agent on Rhodamine Comonomer Addition to Poly(4HPAA)**[a]

| entry | complexing agent | $M_n$ | $M_w$ | $M_p$ | $Đ$ |
|---|---|---|---|---|---|
| poly(4-HPAA) | | 8200 | 16800 | 8500 | 2.05 |
| N-REH | native | 9200 | 16500 | 9500 | 1.79 |
| M-REH | micelle[b] | 13600 | 22800 | 15800[d] | 1.66 |
| H-REH | hydrogel[c] | 10600 | 19300 | 11400 | 1.81 |

[a]Reaction conditions described in Section 2.3.1. [b]PPCMS2.3k-PEG13k-PPCMS2.3k used as complexing agent. [c]PS4.2k-PEG20k-PS4.2k used as complexing agent. [d]Corresponds to addition of 12 comonomer repeating units.

assume that the block copolymers most likely have linear construction.

**3.4. Ibuprofen Conjugated Poly(tyramine)-*b*-poly(4HPAA)-*b*-poly(tyramine).** Modification of poly(tyramine)-*b*-poly(4HPAA)-*b*-poly(tyramine) with ibuprofen was conducted using a maleimide derivative of ibuprofen connected via an ethylenediamine linker. The conjugation was conducted immediately after copolymerization of the poly(tyramine) blocks in the same reaction vessel and was confirmed by $^1$H NMR spectroscopy (Figure 8). The ibuprofen addition was quantified by comparing the signal of the methyl groups of the isobutyl functional group on ibuprofen (1−0.75 ppm) to the aromatic protons (7.3−6.9 ppm). Surprisingly, it was found that both micellar and

**Table 7. Effect of Complexing Agents on Rhodamine Comonomer Addition to Poly(4HPAA)**[a]

| entry | complexing agent | poly(4HPAA) feed (mg) | Rhd-EDA-HPAA feed (mg) | Rhd-EDA-HPAA incorporated (wt %)[b] | quantum yield |
|---|---|---|---|---|---|
| N-REH | native | 60 | 20 | 2.7 | 0.10 |
| M-REH | micelle[c] | 60 | 20 | 18.1 | 0.20 |
| H-REH | hydrogel[d] | 60 | 20 | 8.9 | 0.18 |

[a]Reaction conditions described in Section 2.3.1. [b]Calculated via UV−vis spectroscopy. [c]PPCMS2.3k-PEG13k-PPCMS2.3k used as complexing agent. [d]PS4.2k-PEG20k-PS4.2k used as complexing agent.


https://dx.doi.org/10.1021/acs.biomac.0c00126
Biomacromolecules XXXX, XXX, XXX−XXX

**Scheme 7. Copolymerization of Fluorescein Comonomer with ABA Copolymer**

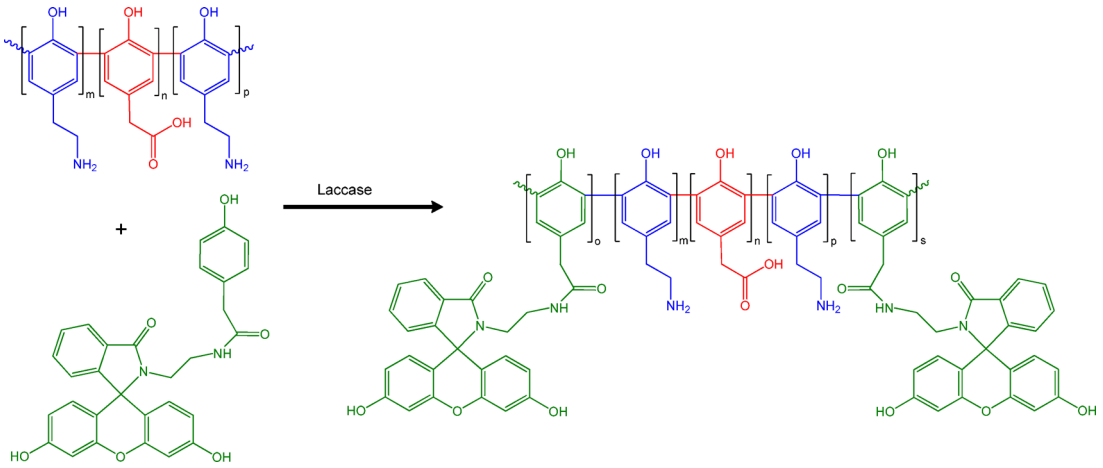


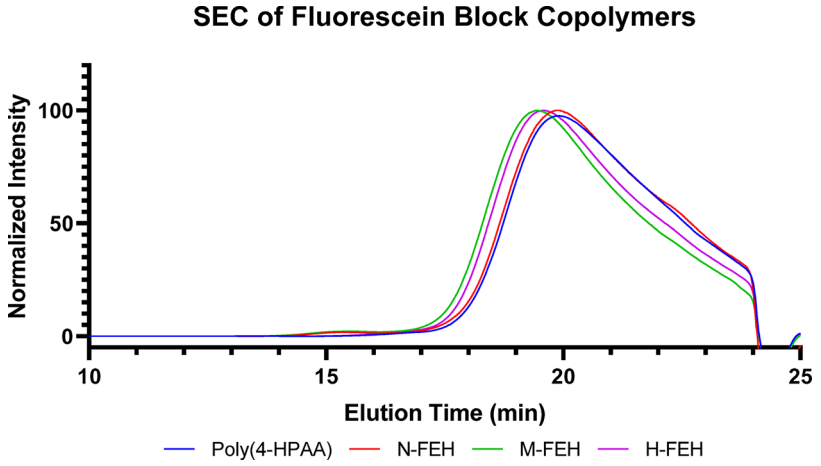


**Figure 9.** SEC traces of poly(Fluor-EDA-HPAA)-*b*-poly(4HPAA)-*b*-poly(Fluor-EDA-HPAA) formed with different complexing agents in 0.1% LiBr DMSO as eluent. See Table 5 for sample designations.

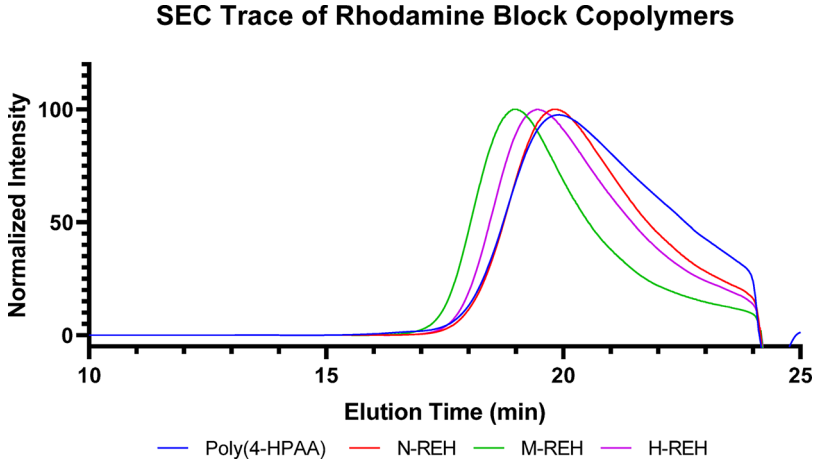


**Figure 10.** SEC traces of poly(4HPAA) (blue) and poly(Rhd-EDA-HPAA)-*b*-poly(4HPAA)-*b*-poly(Rhd-EDA-HPAA) in 0.1% LiBr DMSO as eluent. See Table 7 for sample designations.

hydrogel enzyme complexes reduced the ibuprofen conjugation to the block copolymers (Table 4). This diminished conjugation efficiency was probably caused by the preferential ibuprofen derivative binding to the complexes and therefore having a decreased ability to react with the water-soluble block copolymer. This might initially appear to contradict the rationale for the improved yield and molecular mass of the block copolymers provided in Section 3.1.

It should be noted, however, that the copolymerization of tyramine necessitates interaction of the comonomer with laccase and therefore benefits from the increased local tyramine concentration afforded by the enzyme complexes,


https://dx.doi.org/10.1021/acs.biomac.0c00126
Biomacromolecules XXXX, XXX, XXX−XXX

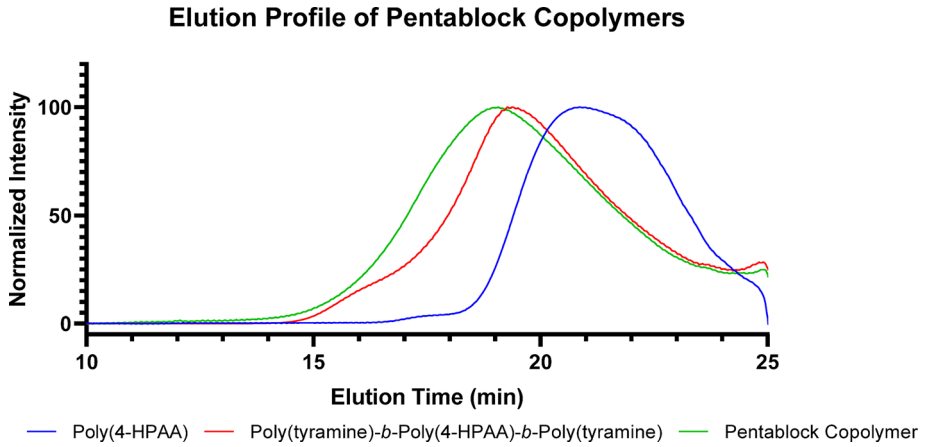


**Figure 11.** SEC trace of poly(4HPAA) (blue), poly(tyramine)-*b*-poly(4HPAA)-*b*-poly(tyramine) (green), and poly(Rhd-EDA-HPAA)-*b*-poly(tyramine)-*b*-poly(4HPAA)-*b*-poly(tyramine)-*b*-poly(Rhd-EDA-HPAA) (yellow) in 0.1% LiBr DMSO as eluent. See Table 9 for sample designations.

**Table 9. Molecular Mass Characteristics of Poly(Fluor-EDA-HPAA)-*b*-poly(tyramine)-*b*-poly(4HPAA)-*b*-poly(tyramine)-*b*-poly(Fluor-EDA-HPAA) Pentablock Copolymer[a]**

| entry | Fluor-EDA-HPAA incorporated[b] (wt %) | $M_n$[c] | $M_w$[c] | $M_p$ | $Đ$[c] |
|---|---|---|---|---|---|
| poly(4-HPAA) | | 6300 | 14100 | 4500 | 2.24 |
| triblock | | 19500 | 43000 | 13000 | 2.19 |
| pentablock[d] | 7.8 ± 1.1 | 29400 ± 2900 | 48700 ± 2000 | 15100 ± 200[e] | 1.65 |

[a]Reaction conditions described in Section 2.3.1. SEC traces of polymers shown in Figure 11. [b]Calculated via UV−vis spectroscopy. [c]Calculated by SEC using PEG standards. [d]Conducted in triplicates. [e]Corresponds to addition of 4 Fluor-ADA-HPAA comonomer repeating units.

**Table 10. Zeta Potential of Poly(4-HPAA), Poly(tyramine)-b-poly(4HPAA)-b-poly(tyramine), and Poly(Fluor-EDA-HPAA)-*b*-poly(tyramine)-*b*-poly(4HPAA)-*b*-poly(tyramine)-*b*-poly(Fluor-EDA-HPAA)**

| sample | zeta potential | std dev |
|---|---|---|
| poly(4HPAA) | −1.84 | 0.601 |
| poly(tyramine)-*b*-poly(4HPAA)-*b*-poly(tyramine) | −20.5 | 1.55 |
| poly(Fluor)-*b*-poly(tyramine)-*b*-poly(4HPAA)-*b*-poly(tyramine)-*b*-poly(Fluor) | −15.2 | 3.94 |

while the coupling of ibuprofen maleimide to tyramine repeating units in the copolymer occurs spontaneously without the need of a catalyst or a complexing agent and therefore suffers from the unfavorable partition coefficient.

**3.5. Synthesis of Fluorescent Triblock Copolymers.** Fluorescent triblock copolymers were successfully produced from the copolymerization of fluorescein and rhodamine 4HPAA derivatives (Scheme 6). The laccase complexes showed seemingly better copolymerization efficiency (increased wt % incorporated), but in general notably lower copolymer molecular masses were observed with the fluorescent comonomers compared to the tyramine triblocks (Tables 6 and 8 vs Table 3). On one side, the lower apparent molecular masses could be caused by distinctly different hydrodynamic volumes of these fluorescent block copolymers affecting their elution time through the SEC separation media. The lower values, however, are most likely the result of both the increased steric hindrance in the bulky comonomers compared to tyramine and their significantly lower water solubility hampering their polyaddition to the reactivated chain ends of poly(4HPAA). Indirect proof of this assumption was provided by the quantum yield of the produced block copolymers (Tables 5 and 7) as reduced incorporation would certainly result in a lower quantum yield. Although the fluorescein comonomer (Fluor-EDA-HPAA) did contain additional phenolic moieties on the fluorescein pendant group, neither fluorescein or fluorescein−ethylenediamine spirolactam polymerized in the presence of laccase. It can therefore be surmised that polymerization of the fluorescein comonomer occurred solely through the phenolic group of the amide linked 4-hydroxyphenylacetamide group.

**3.6. Synthesis of poly(Fluor-EDA-HPAA)-*b*-poly(tyramine)-*b*-poly(4HPAA)-*b*-poly(tyramine)-*b*-poly(Fluor-EDA-HPAA) Pentablock Copolymers.** To further demonstrate the "quasi-living nature" of the developed block copolymerization, pentablock copolymers were synthesized from poly(tyramine)-*b*-poly(4HPAA)-*b*-poly(tyramine) triblock copolymers and the aforementioned Fluor-EDA-HPAA comonomer (Scheme 7).

SEC traces (Figures 9 and 10) of the synthesized block copolymers showed a molecular mass increase indicating the addition of the fluorescein comonomer as exterior blocks (Figure 11). This was further confirmed via UV−vis spectroscopy, which showed the characteristic fluorescein absorption, Table 9.

The relatively large size of the Fluor-EDA-HPAA comonomer is the probable reason for the low copolymerization efficiency (~4 repeating units, Table 9). The notably different hydrodynamic size of the pentablock micelles vs those of the triblock further confirms the attachment of the Fluor-EDA-HPAA comonomer (see DLS traces in Figure S5). The smaller hydrodynamic diameter (58.77 nm, pentablock vs 105.7 nm, triblock) can be explained by the voluminous fluorescein-based blocks decreasing the extent of aggregation (aggregation number). This assumption is also supported by the decrease


https://dx.doi.org/10.1021/acs.biomac.0c00126
Biomacromolecules XXXX, XXX, XXX−XXX

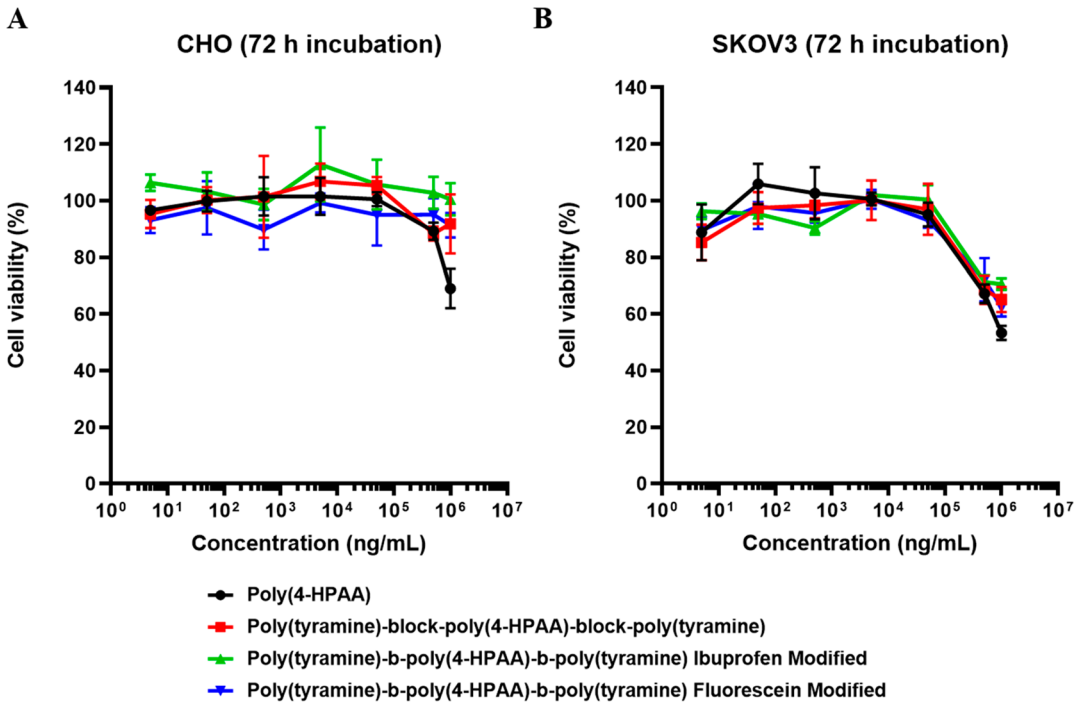


**Figure 12.** Cell viability of CHO (A) and SKOV3 (B) cell lines determined by MTS assays after 72 h incubation with different concentrations of block copolymers.

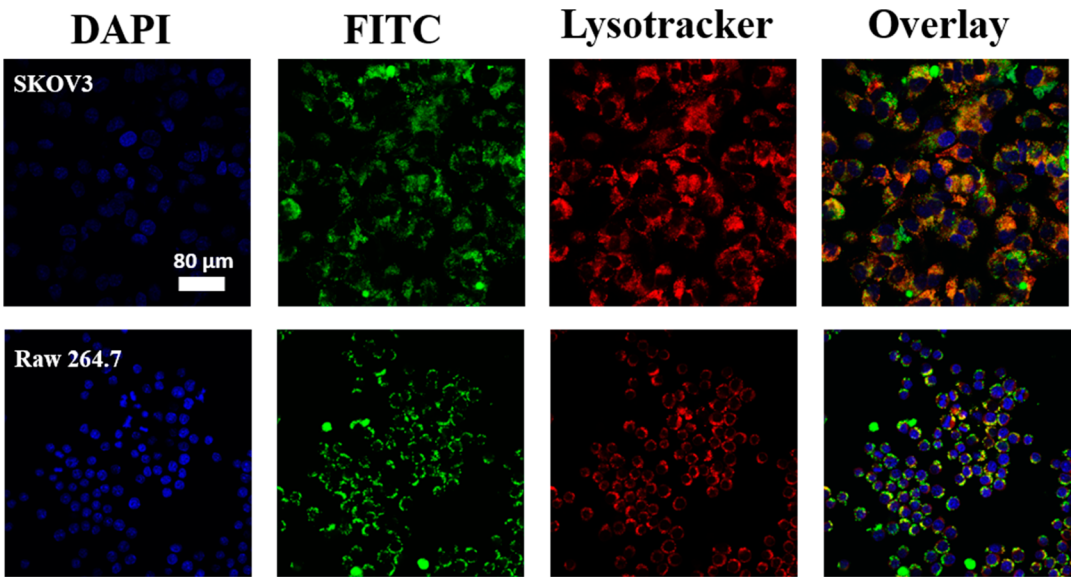


**Figure 13.** Confocal fluorescence microscopy images of SKOV3 ovarian cancer cells and Raw 264.7 macrophage cells incubated with 1 mg/mL of fluorescent fluorescein modified poly(tyramine-*b*-4-hydroxyphenylacetic acid-*b*-tyramine), FITC, for 24 h at 37 °C. The nuclei were stained with DAPI in blue; the green FITC signal revealed the location of fluorescein modified polymers in the cells; the lysosomes were stained with the LysoTracker Red in red color. The scale bar is applicable for all images.

of the pentablocks' zeta potential compared to the triblock precursor (Table 10).

**3.7. Cytotoxicity Studies.** To evaluate the synthesized block copolymers as drug delivery and bioimaging agents, cellular toxicity of the synthesized polymers was determined by MTS assays. Poly(4HPAA), poly(tyramine)-*b*-poly(4HPAA)-*b*-poly(tyramine), and ibuprofen- and fluorescein-modified block copolymers were incubated in the cell cultures of a normal cell line Chinese hamster ovary (CHO) cells and an ovarian cancer SKOV3 cell line, respectively (Figure 12) (protocol described in SI). After 72 h incubation, all these synthetic polymers were observed to be nontoxic on CHO cells at 1 mg/mL concentration except for poly(4HPAA), which exhibited a mild cytotoxicity with 30% reduction of cell viability. In SKOV3 ovarian cancer cell culture, all these block copolymers reduced cell viability to nearly 60% at 1 mg/mL, which may be due to the higher metabolite rates in cancer cells. It was determined in all cases that the polymers were not cytotoxic at concentrations up to 0.5 mg/mL indicating the good biocompatibility of these polymers over a wide concentration range for potential biomedical applications.


https://dx.doi.org/10.1021/acs.biomac.0c00126
Biomacromolecules XXXX, XXX, XXX−XXX

The cell uptake properties of the nanoparticles would define their *in vivo* fate and biodistribution. Cellular uptake of the fluorescein modified poly(tyramine-*b*-4-hydroxyphenylacetic acid-*b*-tyramine), FITC, in SKOV3 ovarian cancer cells and Raw 264.7 macrophage cells was studied *in vitro* using confocal laser scanning microscope. As shown in Figure 13, significant cell uptake of the fluorescent copolymer was observed in the cytosol of both cells, where the FITC signal was colocalized with LysoTracker Red (a fluorescent probe freely permeating cell membranes), indicating an endocytosis pathway for the cell uptake of the nanoparticles. Interestingly, the copolymer was observed to have a greater cell uptake in SKOV-3 ovarian cancer cells than that in Raw 264.7 macrophage cells, which is preferred for the *in vivo* delivery of antitumor drugs without significant clearance by macrophages. In addition, the conjugation of tumor targeting ligands on the functional groups of the copolymer will further improve the tumor targeted drug delivery, which will be tested in the future.

## 4. CONCLUSIONS AND OUTLOOK

Block copolymers composed of 4-hydroxyphenylacetic acid and tyramine were successfully synthesized utilizing a single enzyme catalyzed "quasi-living" copolymerization. To a certain extent the process resembles the "living" polymerization as the polymer formed could continue growing upon introduction of another portion of the same or other monomer and without adding or reactivating the catalyst. In the experiments performed, laccase was first used to polymerize 4-hydroxyphenylacetic acid by a known mechanism (Scheme 1). To the resulting polymer-enzyme solution tyramine was added as the second comonomer and was able to continue polymer propagation onto the poly(4-hydroxphenylacetic acid), which retained reactivity via the freely mobile phenol end groups. Molecular mass of the tyramine blocks was controlled by adjusting comonomer feed. Although limited to phenolic monomers, the reported method is advantageous in that it is not inhibited by irreversible chain termination *via* radical coupling or disproportionation, which are often encountered in the conventional radical polymerization. Additionally, as the initial homopolymerization and the subsequent copolymerization are conducted enzymatically using water as solvent, the described strategy is both environmentally benign and inexpensive. Addition of previously developed micellar and hydrogel complexing agents[34] increased yields by up to 9.4% and 26.0%, respectively, and increased copolymer molecular mass, as well. The utilized enzyme complexes therefore provide an efficient and low cost approach to improve copolymerization efficiency. The scope of the method was further expanded with the successful one-pot synthesis of a pentablock copolymer without any supplementation of additional biocatalyst or complexing agent.

The synthesized block copolymers contain free carboxylic groups on the poly(4-hydroxyphenylacetic acid) interior block imparting high water solubility while the amine groups in the tyramine repeating units provide a facile means of further polymer functionalization. This potential was demonstrated by the efficient attachment of fluorescein and rhodamine derivatives (widely used fluorophores) and ibuprofen, a commonly prescribed anti-inflammatory drug. The theranostic applicability of these multifunctional macromolecules was further confirmed by their low cytotoxicity and preferred cancer cell uptake. These valuable properties make the new multiblock copolymers promising candidates as drug delivery or bioimaging agents and are currently being explored in a separate collaborative effort.

## ■ ASSOCIATED CONTENT

### Supporting Information

The Supporting Information is available free of charge at https://pubs.acs.org/doi/10.1021/acs.biomac.0c00126.

Copolymerization data; SEC and DLS of copolymers, copolymer fluorescence spectra; MALDI-TOF spectra, SEC analysis of copolymerization supernatants, NMR spectra of copolymers produced by post copolymerization modification, enzyme $K_m$ and $V_{max}$ calculation method, cytotoxicity protocol (PDF)

## ■ AUTHOR INFORMATION


### Corresponding Author

**Ivan Gitsov** − *Department of Chemistry, State University of New York − ESF, Syracuse, New York 13210, United States; The Michael M. Szwarc Polymer Research Institute, Syracuse, New York 13210, United States;* orcid.org/0000-0001-7433-8571; Email: igivanov@syr.edu

### Authors

**Dieter Michael Scheibel** − *Department of Chemistry, State University of New York − ESF, Syracuse, New York 13210, United States*

**Dandan Guo** − *Department of Pharmacology, State University of New York Upstate Medical University, Syracuse, New York 13210, United States*

**Juntao Luo** − *Department of Pharmacology, State University of New York Upstate Medical University, Syracuse, New York 13210, United States;* orcid.org/0000-0002-3538-9453

Complete contact information is available at: https://pubs.acs.org/10.1021/acs.biomac.0c00126


### Notes

The authors declare no competing financial interest.

## ■ ACKNOWLEDGMENTS

The authors gratefully acknowledge Dr. Arthur Stipanovic (State University of New York − ESF) for access to SEC instrumentation. Partial funding for this study was provided by State University of New York Network of Excellence on Materials and Advanced Manufacturing (Award 1126892-1-71036 to I.G.).

## ■ REFERENCES


(1) Szwarc, M. 'Living' Polymers. *Nature* **1956**, *178*, 1168−1169.

(2) Szwarc, M. Living Polymers. Their Discovery, Characterization, and Properties. *J. Polym. Sci., Part A: Polym. Chem.* **1998**, *36*, No. ix.

(3) Smid, J. Historical perspectives of living anionic polymerization. *J. Polym. Sci., Part A: Polym. Chem.* **2002**, *40*, 2101−2107.

(4) Mai, Y.; Eisenberg, A. Self-assembly of block copolymers. *Chem. Soc. Rev.* **2012**, *41*, 5969−5985.

(5) Wei, H.; Cheng, S.-X.; Zhang, X.-Z.; Zhuo, R.-X. Thermosensitive polymeric micelles based on poly(n-isopropylacrylamide) as drug carriers. *Prog. Polym. Sci.* **2009**, *34*, 893−910.

(6) Wang, J.; Yao, K.; Wang, C.; Tang, T.; Jiang, X. Synthesis and drug delivery of novel amphiphilic block copolymers containing hydrophobic dehydroabietic moiety. *J. Mater. Chem. B* **2013**, *1*, 2324−2332.

(7) Rosler, A.; Vandermeulen, G. W.; Klok, H.-A. Advanced drug delivery devices via self-assembly of amphiphilic block copolymers. *Adv. Drug Delivery Rev.* **2012**, *64*, 270−279.
(8) Bates, C. M.; Maher, M. J.; Janes, D. W.; Ellison, C. J.; Willson, C. G. Block copolymer lithography. *Macromolecules* **2014**, *47*, 2−12.
(9) Schulze, M. W.; McIntosh, L. D.; Hillmyer, M. A.; Lodge, T. P. High-modulus, high-conductivity nanostructured polymer electrolyte membranes via polymerization-induced phase separation. *Nano Lett.* **2014**, *14*, 122−126.
(10) Upadhyaya, L.; Semsarilar, M.; Fernandez-Pacheco, R.; Martinez, G.; Mallada, R.; Deratani, A.; Quemener, D. Porous membranes from acid decorated block copolymer nano-objects via RAFT alcoholic dispersion polymerization. *Polym. Chem.* **2016**, *7*, 1899−1906.
(11) Saleem, S.; Rangou, S.; Abetz, C.; Lademann, B.; Filiz, V.; Abetz, V. Block Copolymer Membranes from Polystyrene-*b*-poly(solketal methacrylate) (PS-*b*-PSMA) and Amphiphilic Polystyrene-*b*-poly(glyceryl methacrylate) (PS-*b*-PGMA). *Polymers* **2017**, *9*, 216.
(12) Liu, X.; Monzavi, T.; Gitsov, I. Controlled ATRP Synthesis of Novel Linear-Dendritic Block Copolymers and Their Directed Self-Assembly in Breath Figure Arrays. *Polymers* **2019**, *11* (3), 539.
(13) Kato, M.; Kamigaito, M.; Sawamoto, M.; Higashimura, T. Polymerization of Methyl Methacrylate with the Carbon Tetrachloride/Dichlorotris-(triphenylphosphine)ruthenium(II)/Methylaluminum Bis(2,6-di-tert-butylphenoxide) Initiating System: Possibility of Living Radical Polymerization. *Macromolecules* **1995**, *28*, 1721−1723.
(14) Wang, J.-S.; Matyjaszewski, K. Controlled/"living" radical polymerization. Atom transfer radical polymerization in the presence of transition-metal complexes. *J. Am. Chem. Soc.* **1995**, *117*, 5614−5615.
(15) Chiefari, J.; Chong, Y. K.; Ercole, F.; Krstina, J.; Jeffery, J.; Le, T. P. T.; Mayadunne, R. T. A.; Meijs, G. F.; Moad, C. L.; Moad, G.; Rizzardo, E.; Thang, S. H. Living Free-Radical Polymerization by Reversible Addition-Fragmentation Chain Transfer: The RAFT Process. *Macromolecules* **1998**, *31*, 5559.
(16) Georges, M. K.; Veregin, R. P. N.; Kazmaier, P. M.; Hamer, G. K. Narrow molecular weight resins by a free-radical polymerization process. *Macromolecules* **1993**, *26*, 2987−2988.
(17) Davis, K. A.; Matyjaszewski, K. ABC Triblock Copolymers Prepared Using Atom Transfer Radical Polymerization Techniques. *Macromolecules* **2001**, *34*, 2101−2107.
(18) Miletic, N.; Nastasovic, A.; Loos, K. Immobilization of biocatalysts for enzymatic polymerizations: possibilities, advantages, applications. *Bioresour. Technol.* **2012**, *115*, 126−135.
(19) Lewis, J. C.; Coelho, P. S.; Arnold, F. H. Enzymatic functionalization of carbon-hydrogen bonds. *Chem. Soc. Rev.* **2011**, *40*, 2003−2021.
(20) Davis, B. G.; Boyer, V. Biocatalysis and enzymes in organic synthesis. *Nat. Prod. Rep.* **2001**, *18*, 618−640.
(21) Bisht, K. S.; Henderson, L. A.; Gross, R. A.; Kaplan, D. L.; Swift, G. Enzyme-Catalyzed Ring-Opening Polymerization of ω-Pentadecalactone. *Macromolecules* **1997**, *30*, 2705−2711.
(22) Soeda, Y.; Okamoto, T.; Toshima, K.; Matsumura, S. Enzymatic Ring-Opening Polymerization of Oxiranes and Dicarboxylic Anhydrides. *Macromol. Biosci.* **2002**, *2*, 429−436.
(23) Sigg, S.; Seidi, F.; Renggli, K.; Silva, T.; Kali, G.; Bruns, N. Horseradish Peroxidase as a Catalyst of Atom Transfer Radical Polymerization. *Macromol. Rapid Commun.* **2011**, *32*, 1710−1715.
(24) Duxbury, C. J.; Wang, W.; de Geus, M.; Heise, A.; Howdle, S. M. Can Block Copolymers be synthesized by a Single-Step Chemoenzymatic Route in Supercritical Carbon Dioxide? *J. Am. Chem. Soc.* **2005**, *127*, 2384−2385.
(25) Liu, Z.; Lv, Y.; An, Z. Enzymatic Cascade Catalysis for the Synthesis of Multiblock and Ultrahigh-Molecular-Weight Polymers with Oxygen Tolerance. *Angew. Chem., Int. Ed.* **2017**, *56*, 13852−13856.
(26) Ikeda, R.; Tanaka, H.; Uyama, H.; Kobayashi, S. Laccase-catalyzed polymerization of acrylamide. *Macromol. Rapid Commun.* **1998**, *19*, 423−425.
(27) Mita, N.; Tawaki, S.-i.; Uyama, H.; Kobayashi, S. Laccase-Catalyzed Oxidative Polymerization of Phenols. *Macromol. Biosci.* **2003**, *3*, 253−257.
(28) Kashima, K.; Fujisaki, T.; Serrano-Luginbühl, S.; Kissner, R.; Janošević Ležaić, A.; Bajuk-Bogdanović, D.; ćirić-Marjanović, G.; Busato, S.; Ishikawa, T.; Walde, P. Effect of Template Type on the *Trametes versicolor* Laccase-Catalyzed Oligomerization of the Aniline Dimer *p*-Aminodiphenylamine (PADPA). *ACS Omega* **2019**, *4*, 2931−2947.
(29) Cannatelli, M. D.; Ragauskas, A. J. Two Decades of Laccases: Advancing Sustainability in the Chemical Industry. *Chem. Record* **2017**, *17*, 122−140.
(30) Mate, D. M.; Alcalde, M. Laccase: a multipurpose biocatalysts at the forefront of biotechnology. *Microb. Biotechnol.* **2017**, *10*, 1457−1467.
(31) Gitsov, I.; Wang, L.; Vladimirov, N.; Simonyan, A.; Kiemle, D. J.; Schutz, A. Green" Synthesis of Unnatural Poly(Amino Acid)s with Zwitterionic Character and pH-Responsive Solution Behavior, Mediated by Linear-Dendritic Laccase Complexes. *Biomacromolecules* **2014**, *15*, 4082−4095.
(32) Papadopoulos, G.; Boskou, D. Antioxidant effect of natural phenols on olive oil. *J. Am. Oil Chem. Soc.* **1991**, *68*, 669−671.
(33) Smith, T. A. Phenethylamine and related compounds in plants. *Phytochemistry* **1977**, *16*, 9−18.
(34) Scheibel, D.; Gitsov, I. Polymer-Assisted Biocatalysis: Effects of Macromolecular Architectures on the Stability and Catalytic Activity of Immobilized Enzymes toward Water-Soluble and Water-Insoluble Substrates. *ACS Omega.* **2018**, *3*, 1700−1709.
(35) Kalyanasundaram, K.; Thomas, J. K. Environmental effects on vibronic band intensities in pyrene monomer fluorescence and their application in studies of micellar systems. *J. Am. Chem. Soc.* **1977**, *99*, 2039−2044.


https://dx.doi.org/10.1021/acs.biomac.0c00126
*Biomacromolecules* XXXX, XXX, XXX−XXX